

# Breath Analysis for the In Vivo Detection of Diabetic Ketoacidosis

Mizaj Shabil Sha,<sup>▽</sup> Muni Raj Maurya,<sup>▽</sup> Sadiyah Shafath, John-John Cabibihan, Abdulaziz Al-Ali, Rayaz A. Malik, and Kishor Kumar Sadasivuni\*



Cite This: *ACS Omega* 2022, 7, 4257–4266



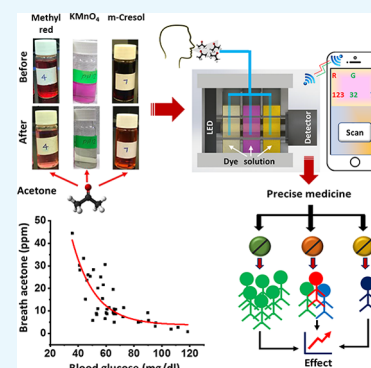
Read Online

ACCESS |

Metrics & More

Article Recommendations

**ABSTRACT:** Human breath analysis of volatile organic compounds has gained significant attention recently because of its rapid and noninvasive potential to detect various metabolic diseases. The detection of ketones in the breath and blood is key to diagnosing and managing diabetic ketoacidosis (DKA) in patients with type 1 diabetes. It may also be of increasing importance to detect euglycemic ketoacidosis in patients with type 1 or type 2 diabetes or heart failure, treated with sodium-glucose transporter-2 inhibitors (SGLT2-i). The present research evaluates the efficiency of colorimetry for detecting acetone and ethanol in exhaled human breath with the response time, pH effect, temperature effect, concentration effect, and selectivity of dyes. Using the proposed multidye system, we obtained a detection limit of 0.0217 ppm for acetone and 0.029 ppm for ethanol in the detection range of 0.05–50 ppm. A smartphone-assisted unit consisting of a portable colorimetric device was used to detect relative red/green/blue values within 60 s of the interface for practical and real-time application. The developed method could be used for rapid, low-cost detection of ketones in patients with type 1 diabetes and DKA and patients with type 1 or type 2 diabetes or heart failure treated with SGLT2-I and euglycemic ketoacidosis.



## 1. INTRODUCTION

Diabetic ketoacidosis (DKA) is an acute metabolic complication in type 1 diabetes mellitus and is associated with increased morbidity and mortality, especially when the diagnosis and treatment are delayed.<sup>1</sup> This is particularly relevant in resource-limited settings when patients with limited access to insulin and healthcare systems due to financial constraints present in severe ketoacidosis. The risk of DKA is also increased in patients with renal failure, during pregnancy, and in patients during fasting.<sup>2,3</sup> Sodium-glucose cotransporter-2 inhibitors have emerged as a highly effective treatment in patients with diabetes<sup>4</sup> and heart failure<sup>5</sup> with benefits on glycemia, renal function,<sup>6</sup> cardiovascular outcomes, and all-cause mortality.<sup>7,8</sup> However, of concern, they have been associated with a twofold increase in the risk of developing ketoacidosis.<sup>9</sup>

The conventional method used to detect ketoacidosis requires a blood sample and access to a laboratory to measure the concentration of serum  $\beta$ -hydroxybutyrate.<sup>10</sup> Noninvasive and minimally invasive techniques, including radio-wave impedance, infrared spectroscopy, optical rotation of polarized light, and biosensors, have been proposed for monitoring blood glucose.<sup>11</sup> Another emerging noninvasive technique is monitoring exhaled breath as it contains numerous bio-products arising from physiological enzyme reactions.<sup>12</sup> Acetone and ethanol are excellent examples of metabolic products which can act as markers of altered pathophysiology

in patients with diabetes.<sup>13,14</sup> Breath analysis is rapid, noninvasive, and repeatable for long-term clinical monitoring.

The “fruity odor” of ketones on a patient’s breath with ketoacidosis has been used clinically for many years.<sup>15,16</sup> However, accurate quantitative breath analysis may enable rapid, noninvasive, and repeatable monitoring of ketoacidosis.<sup>17</sup> An acetone breath concentration of <0.9 ppm is normal, and a concentration >1.7 ppm indicates ketoacidosis.<sup>18,19</sup>

The current study aims to evolve a low-cost detection method using a multidye system for the accurate and precise colorimetric sensing of acetone/ethanol as a bioindicator for detecting DKA. Compared to the other analytical methods, the colorimetric assay has received considerable attention due to its simplicity, rapid execution, and low cost.<sup>20,21</sup> Wang et al. developed a colorimetric sensor to detect breath acetone by incorporating hydroxylamine sulfate and thymol blue in a porous substrate.<sup>21</sup> However, it is only of one-time use and strictly depends on the visible color change produced by the reaction. It cannot quantify the concentration from exhaled breath, which is key to identifying the severity of disease, and

**Received:** October 24, 2021

**Accepted:** January 10, 2022

**Published:** January 24, 2022



the limit of detection (LOD) and temperature effect of the sensor have not been analyzed.

The current device has multiple dyes for accurate breath acetone and ethanol measurement at different temperatures. Additionally, this highly selective and sensitive colorimetric sensor has a smartphone-assisted unit to estimate relative red/green/blue (RGB) values within 1 min, enabling the visual assessment of biomarker concentration. Our sensor has applications in health and can also be used for forensic purposes and water treatment and purification techniques.

## 2. RESULTS AND DISCUSSION

This study made novel observations regarding quantifying breath ethanol and acetone in human subjects. The liver converts circulating free fatty acids to acetyl-coenzyme A (acetyl-CoA) which condenses with oxaloacetate, and enters the TCA cycle. When glucose availability is reduced due to fasting or a low-carbohydrate diet, insulin deficiency, or insulin resistance, the production of acetyl CoA from fatty acids increases with increased ketone bodies, leading to increased blood and breath acetone concentration.<sup>17,22</sup>

In the case of ethanol, there is no direct biochemical pathway to produce it in humans. Excessive carbohydrate-rich food can lead to small amounts of ethanol (3 ppm) generation by intestinal bacteria or yeast in humans with unusual yeast or bacterial populations due to prolonged antibiotic use, poor nutrition, or very high carbohydrate diets; massive fermentation and ethanol production result in the “autobrewery syndrome or drunkenness disease”, leading to increased blood alcohol concentration with intoxication without consuming alcohol.<sup>23</sup> The metabolism of bacteria or yeast accompanies anaerobic metabolism to pyruvate, which is transformed to acetaldehyde via pyruvate decarboxylase and converted to ethanol by alcohol dehydrogenase (ADH).<sup>24</sup> A physiological role of ADH is to rid the body of any ethanol produced by the fermentation of sugars in the gut during a process known as first-pass metabolism and provides a detoxification mechanism whenever ethanol is inadvertently ingested together with fermented fruit juices, honey, and sugar. Indeed, endogenous ethanol may increase in diabetic patients without alcohol consumption.

To construct a highly sensitive colorimetric volatile organic compound sensor, both acetone and ethanol (concentration varying from 0.05 to 50 ppm) were added to the dye solutions in an acidic, basic, and neutral medium and observed for any visible color change. In addition, the response time, pH effect, temperature effect, concentration effect, and selective nature of the dyes were studied and analyzed.

The list of notations used is explained in Table 1. Here,  $P$  represents the pH, whereas  $x$  denotes the specific pH,  $T$  represents the temperature, and  $y$  stands for a particular temperature.  $Z$  stands for the concentration of the biomarker [acetone (A) and ethanol (E)].

**2.1. Response Time and pH Effect.** For the assay, 1 mL of the biomarker (acetone/ethanol) solution along with a 0.05–50 ppm concentration was added to the dye solutions with the pH values of 2, 4, 6, 7, 9, and 12 at room temperature. The response time for the dyes was estimated by calculating the time from the addition of the biomarker to the corresponding visible color change observed in the dye solution. Potassium permanganate, methyl red, and *m*-cresol purple successfully detected acetone (Table 2). Moreover, irrespective of the pH value, each dye response time decreased

**Table 1. List of Notations Used**

dyes	dye indication	specific pH ( $P_x$ ), specific temperature ( $T_y$ in °C), and biomarker [acetone (A)/ethanol (E)] – concentration ( $z$ in ppm) indication
KMnO <sub>4</sub>	KM	KM( $P_xT_yAz$ )
<i>m</i> -cresol purple	CP	CP( $P_xT_yAz$ )
methyl orange	MO	MO( $P_xT_yEz$ )
methyl red	MR	MR( $P_xT_yAz$ ), MR( $P_xT_yEz$ )
iodoform test	IF	IF( $P_xT_yEz$ )

**Table 2. Colorimetric Detection of Acetone Using Different Dyes**

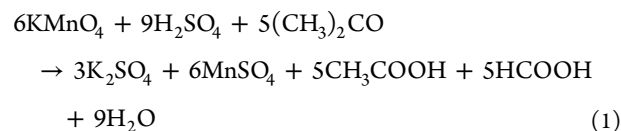
sl. no	dye solution–acetone mixture	average response time (min)
1	MR( $P_4T_2SAz$ )	15
2	KM( $P_{12}T_2SAz$ )	8
3	CP( $P_7T_2SAz$ )	10

with an increase in the acetone concentration. Figure 1a,b shows the color change in the methyl red dye solution after adding 5 ppm acetone. From Figure 1a, it can be inferred that the pH 4 dye solution color tends to diminish with acetone. It can be concluded that the color reaction of methyl red and acetone can be completed within 15 min for acetone concentrations as low as 0.5 ppm. The emergence of a new absorption band centered at ~554 nm with a.u.~0.1893 from ~550 nm (a.u.~0.7459) was observed in the UV–vis absorbance spectra (Figure 1b).

For the acetone assay in the *m*-cresol purple solution, a visible color change was noticed in the neutral solution for all acetone concentrations, that is, 0.5–50 ppm. Figure 1c shows the color change in the *m*-cresol purple solution after the addition of 5 ppm acetone. An apparent visible color change from brick red to light red was observed in the dye solution of pH 7. The response time of the pH 7 solution increased with a decrease in the acetone concentration, and the average response time was estimated to be 10 min. The peak in the UV analysis (Figure 1d) exhibited a shift from 504 nm (a.u. ~ 0.2369) to 498 nm (a.u. ~ 0.99499).

Figure 1e shows the color change in the KMnO<sub>4</sub> solution after adding 5 ppm acetone. An apparent visible color change from violet to the colorless solution is observed in the dye solution of pH 12, along with a change in the intensity from a.u. of 1.18 to 1.0079 (Figure 1f). The observable color change can be distinguished at a concentration of acetone as low as 0.5 ppm, offering a convenient approach to detect acetone by the unaided eye.

An example of the reaction of dyes with acetone is given below



Equation 1 represents the reaction of KMnO<sub>4</sub> with acetone. The products generated are potassium sulfate, manganese sulfate, acetic acid, and formic acid.

Both methyl orange and methyl red detected ethanol. UV–vis analysis showed that these two dyes could detect ethanol

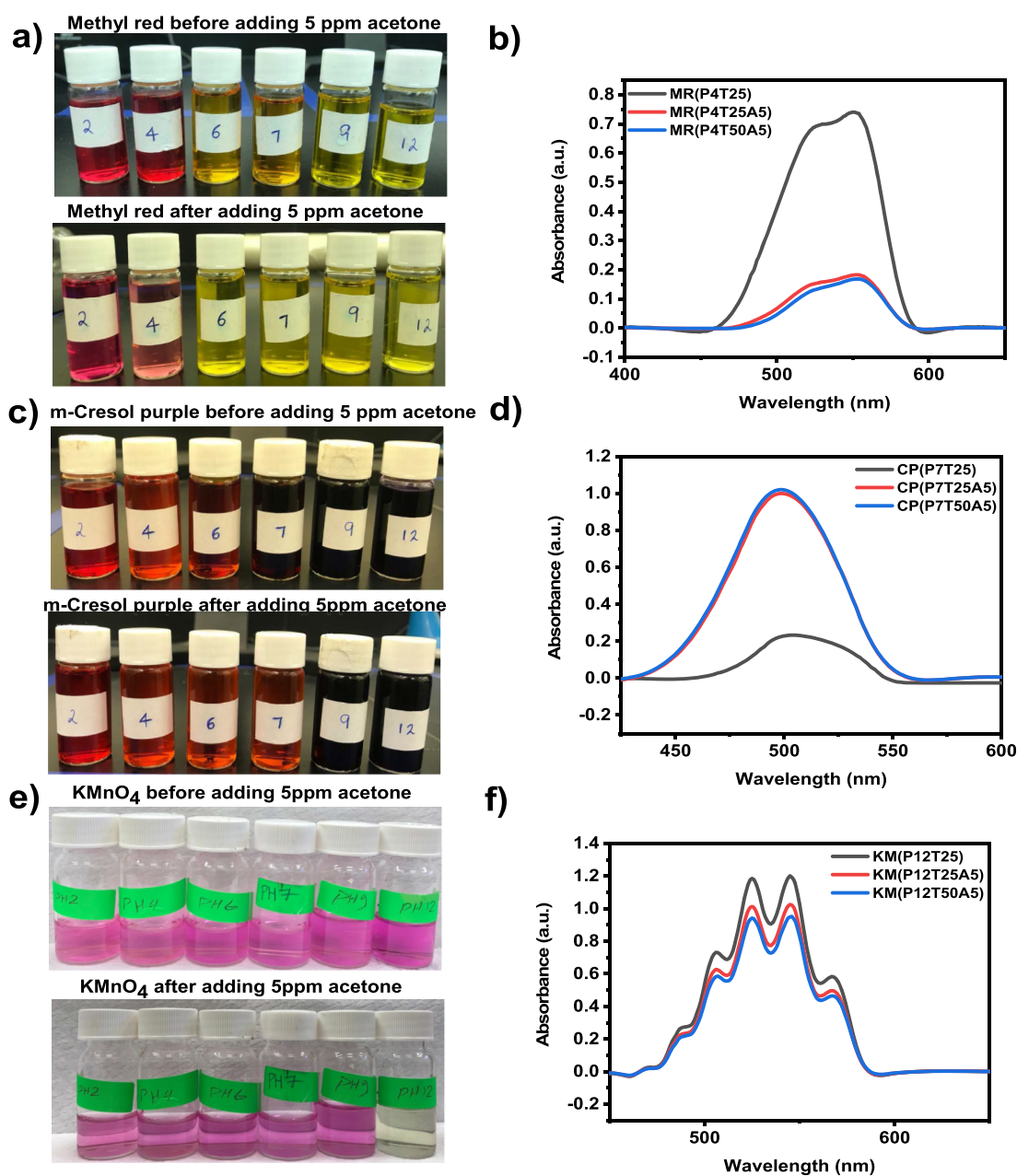


**Figure 1.** Acetone detection by different dyes. (a) pH-adjusted methyl red dye solution at room temperature before and after adding 5 ppm acetone. (b) UV-vis absorbance spectra of the pH 4 methyl red dye solution at different temperatures. (c) pH-adjusted *m*-cresol purple dye solution at room temperature before and after adding 5 ppm acetone. (d) UV-vis absorbance spectra of the pH 7 *m*-cresol purple dye solution at different temperatures. (e) pH-adjusted KMnO<sub>4</sub> dye solution at room temperature before and after adding 5 ppm acetone. (f) UV-vis absorbance spectra of the pH 12 KMnO<sub>4</sub> dye solution at different temperatures.

(Figure 2). Methyl orange detected ethanol in neutral and basic solutions, whereas methyl red responded in acidic and pH 9 solutions. Figure 2 represents a slight change in absorbance for both the dyes. For methyl orange, a new peak was centered at 487 nm with a.u.  $\sim 0.577$ , and initially, the peak was centered at 508 nm with a.u.  $\sim 0.159$ . In the case of methyl red, change was observed from 553 nm (a.u.  $\sim 1.504$ ) to 550 nm (a.u.  $\sim 1.344$ ). Here, along with colorimetry, we used the iodoform test to detect ethanol. In the iodoform test, the presence of carbonyl compounds with the structure R-CO-CH<sub>3</sub> or alcohols with the structure R-CH(OH)-CH<sub>3</sub> can be recognized. The reaction of iodine with a base in a methyl ketone gives a yellow precipitate with an antiseptic

odor. Ethanol is the only primary alcohol that responds to the iodoform test.

The product formed in this test is iodoform or triiodomethane. It can be used to identify aldehydes or ketones. If an aldehyde gives a positive result in the iodoform test, it must be acetaldehyde since it is the only aldehyde with a CH<sub>3</sub>C=O group.

**2.2. Sensitivity Analysis and the LOD of Dye Solutions.** The dyes' concentration effect was analyzed with different test solution concentrations (0.05–50 ppm) added to dye solutions at ambient temperature (Figure 3). While investigating the impact of the concentration, it was observed that color change took place faster when the test solution was

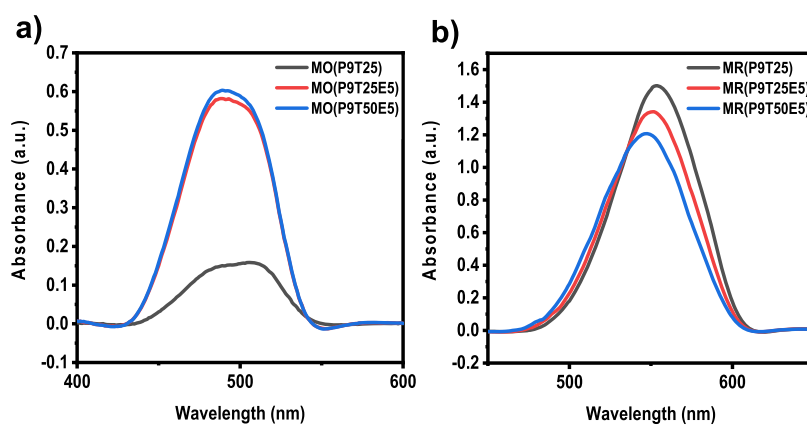


Figure 2. Response to 5 ppm ethanol by pH 9 dye solutions (a) methyl orange and (b) methyl red.

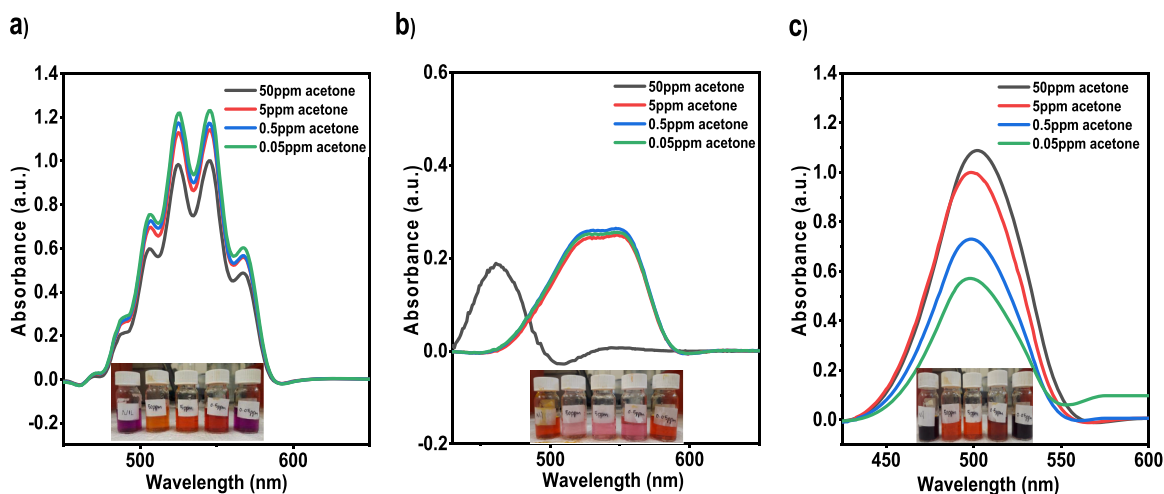


Figure 3. Sensitivity analysis of acetone with concentrations 0.05–50 ppm in (a)  $\text{KMnO}_4$ , (b) methyl red, and (c) *m*-cresol purple, respectively.

of a higher concentration for all the dye solutions. As per the Beer–Lambert law, the concentration and absorbance of the solution exhibit a linear relationship, which could be used to predict the concentration of a solution by measuring its absorbance. A linear calibration curve of the absorbance versus concentration was plotted (Figure 4).

The calibration curve was plotted by considering the peak absorbance of the dye, and a linear fitting was performed to estimate the LOD using the  $3\sigma/m$  criterion, where  $m$  is the slope of the calibration plot and  $\sigma$  is the standard deviation of the intercept. Figure 4a–c shows the calibration curve for acetone, and Figure 4d–f shows the calibration curve for ethanol, respectively. The estimated LOD of  $\text{KMnO}_4$  was 0.045 ppm [ $y = (0.387)x + (0.88611 \pm 0.0059)$ ;  $R^2 = 0.99266$ ]. Like  $\text{KMnO}_4$ , the calibration curve was plotted from 0.05 to 50 ppm for methyl red. The linear fit to the data revealed an LOD of  $\sim 0.0217$  ppm toward acetone sensing by the methyl red dye [ $y = (0.7983)x + (0.2242 \pm 0.00258)$ ;  $R^2 = 0.96806$ ]. Similarly, the linear fitting was performed in the range of 0.05–50 ppm acetone for cresol purple and the estimated LOD of the dye was  $\sim 0.026$  ppm [ $y = (0.726)x + (0.73746 \pm 0.00653)$ ;  $R^2 = 0.99745$ ]. The sensitivity investigation indicates that these three dye systems exhibit high sensitivity toward acetone with a detection limit as low as  $\sim 0.0217$  ppm.

In the case of ethanol, the linear fitting was performed in the range of 0.05–50 ppm and the estimated LOD of methyl

orange was 0.0496 ppm [ $y = (0.0302)x + (0.44931 \pm 0.00505)$ ;  $R^2 = 0.99122$ ]. Similarly, the linear fitting for ethanol estimated a LOD of methyl red dye as 0.05 ppm [ $y = (0.305)x + (1.1723 \pm 0.00509)$ ;  $R^2 = 0.9913$ ]. For the iodoform test, the LOD is 0.029 ppm [ $y = (0.8321)x + (0.42344 \pm 0.008122)$ ;  $R^2 = 0.99699$ ]. The sensitivity investigation indicates that these three systems exhibit high sensitivity toward ethanol with a detection limit as low as  $\sim 0.029$  ppm.

**2.3. Temperature Effect.** A key property for any biosensor is that it should possess the stability of the sensing system toward a change in the temperature of the surrounding medium. Along with an effect on dye system stability, the temperature also affects the physical dimension of the molecule. The thermodynamic aspect is that a temperature rise increases the vapor pressure and reduces the response and sensitivity. Thus, the temperature should have a negligible impact on an excellent sensing system.

To investigate this parameter, the dye solutions were heated at different temperatures, that is, 25, 50, 75, and 100 °C and a 1 mL test solution with a concentration of 5 ppm was added to the dye solutions. For all dye solutions, the intensity of absorption remained almost constant, irrespective of the change in the temperature (Figure 5). Analysis showed that  $\text{KMnO}_4$  has an absorbance variation of  $1 \pm 0.003$ , whereas, for methyl red, the variation was from  $0.90525 \pm 0.001$ . Similarly, cresol purple exhibited a change in absorbance close to  $0.99 \pm 0.002$ . In the case of ethanol, the absorption variations for

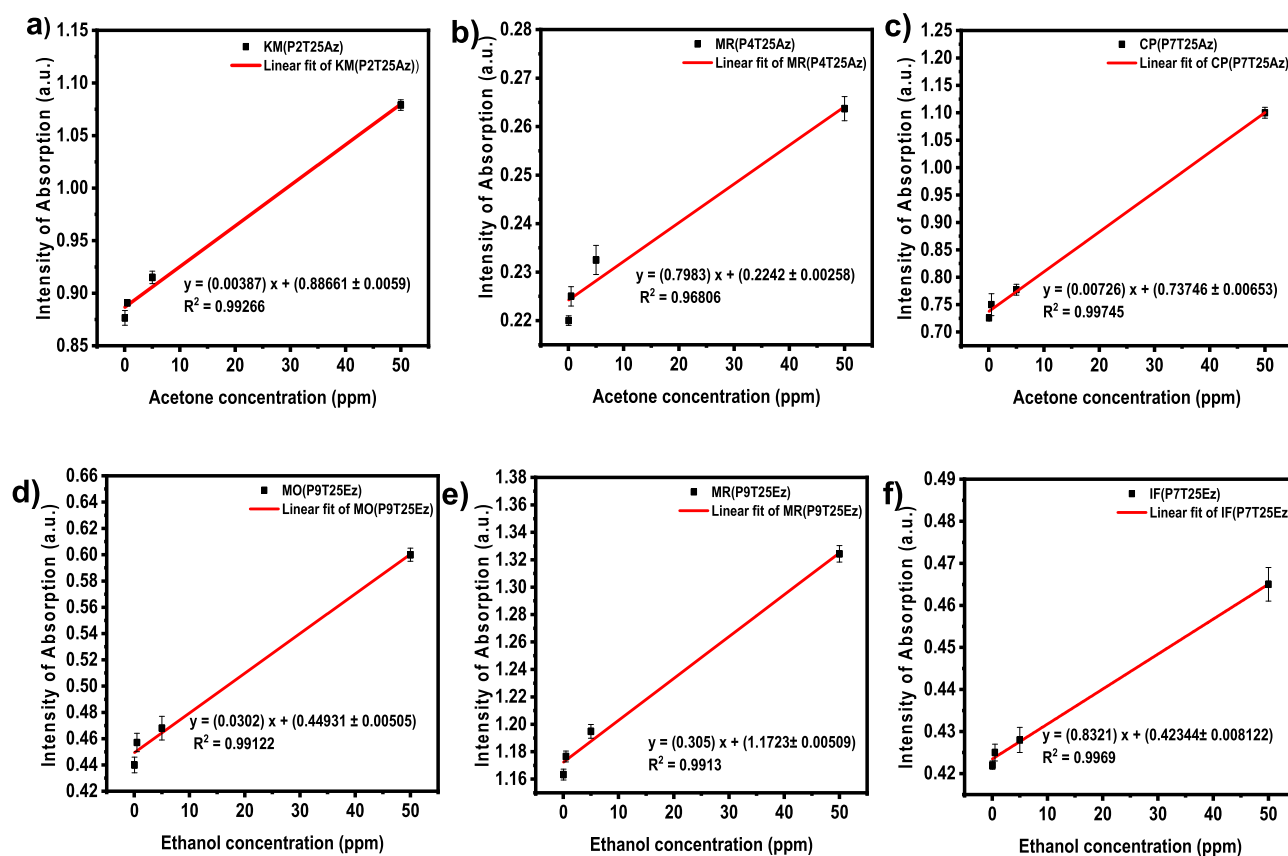


**Figure 4.** Calibration plot of acetone in (a)  $\text{KMnO}_4$ , (b) methyl red, and (c) *m*-cresol purple. Calibration plot of ethanol in (d) methyl orange, (e) methyl red, and (f) iodoform test.

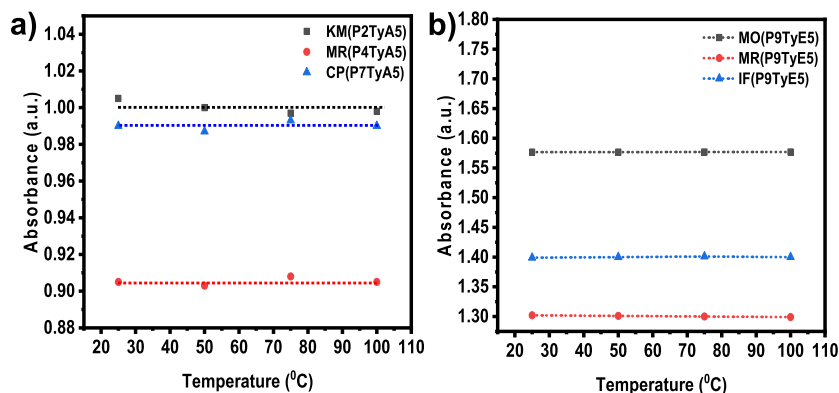


**Figure 5.** Temperature effect of biomarkers in dye solutions: (a) acetone in temperature-adjusted dye solutions (25, 50, 75, and 100 °C) and (b) ethanol in temperature-adjusted dye solutions (25, 50, 75, and 100 °C).

methyl orange, methyl red, and iodoform were  $1.5767 \pm 0.0008$ ,  $1.3005 \pm 0.00001$ , and  $1.4 \pm 0.007$ , respectively. This indicates that the multisensor system is highly stable, which is desirable for the real-time application of the proposed colorimetric sensor.

**2.4. Selectivity Analysis.** To ensure the selectivity and specificity of the sensor, various test solutions representing other biomarkers in breath such as ammonia, benzene, formaldehyde, hydrogen peroxide, nitric oxide, and toluene were also added in the dye solutions. The test analyte had a concentration of 5 ppm, and a test was carried out for dye solutions at room temperature, followed by UV–vis analysis. The results showed that all dye solutions apprehended an incredible selective nature toward acetone/ethanol.

The dye's selectivity for acetone/ethanol was confirmed by measuring the relative change in the wavelength ( $\Delta\lambda$ ) from UV–vis analysis estimated by the equation given below.

$$\Delta\lambda = \frac{\lambda_x - \lambda_0}{\lambda_0} \times 100 \quad (2)$$

where  $\lambda_x$  is the specific wavelength of peak absorbance in the presence of the analyte and  $\lambda_0$  is the wavelength of maximum absorbance of the blank solution. The  $\Delta\lambda$  value is estimated at pH 12, pH 7, pH 7, and pH 4 for  $\text{KMnO}_4$ , *m*-cresol purple, methyl orange, and methyl red dyes. The dye solutions detected the corresponding biomarkers only (Figure 6). These results indicate that other interfering substances showed weak

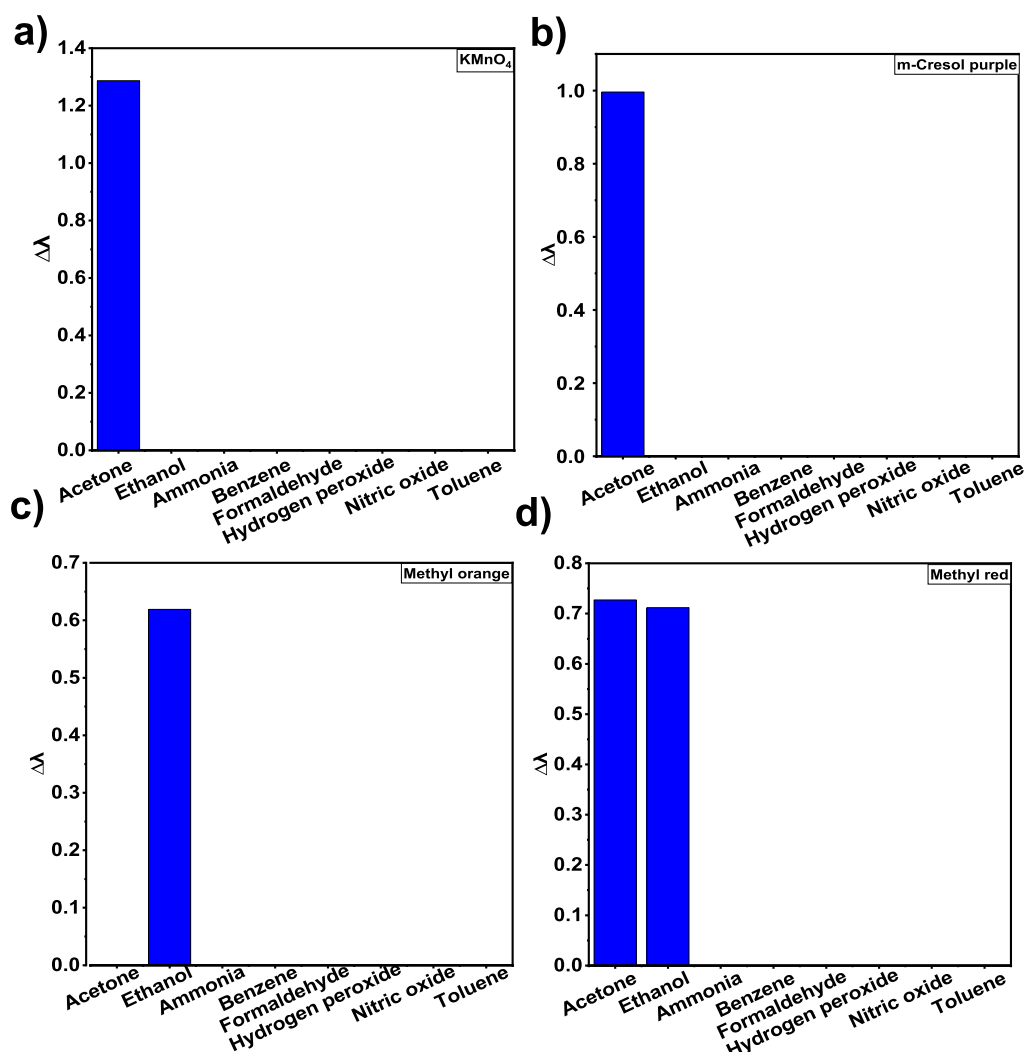


**Figure 6.** Selectivity analysis of biomarkers in different dye solutions: (a)  $KMnO_4$  dye solutions, (b) *m*-cresol purple, (c) methyl orange, and (d) methyl red.

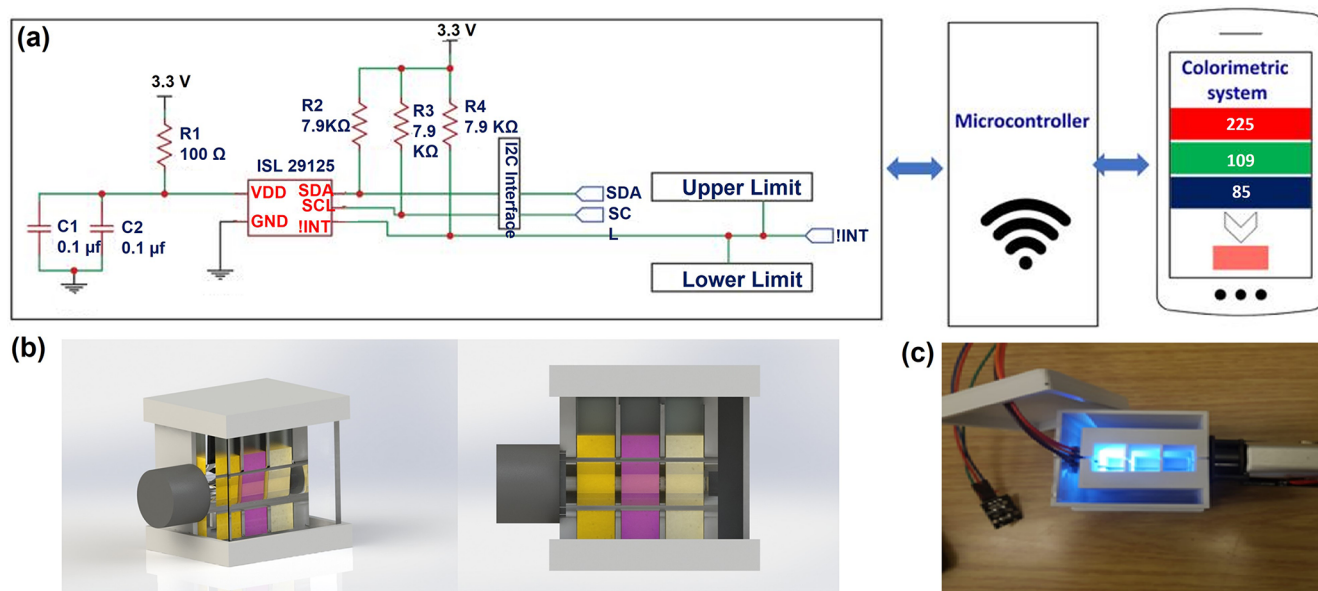


**Figure 7.** (a) Schematic of the fabricated sensor prototype, illustrating that the dye system triggered a colorimetric array and smartphone-interfaced unit to detect acetone/ethanol levels. (b) 3D image of the proposed sensor prototype. (c) Real image of the developed sensor prototype.

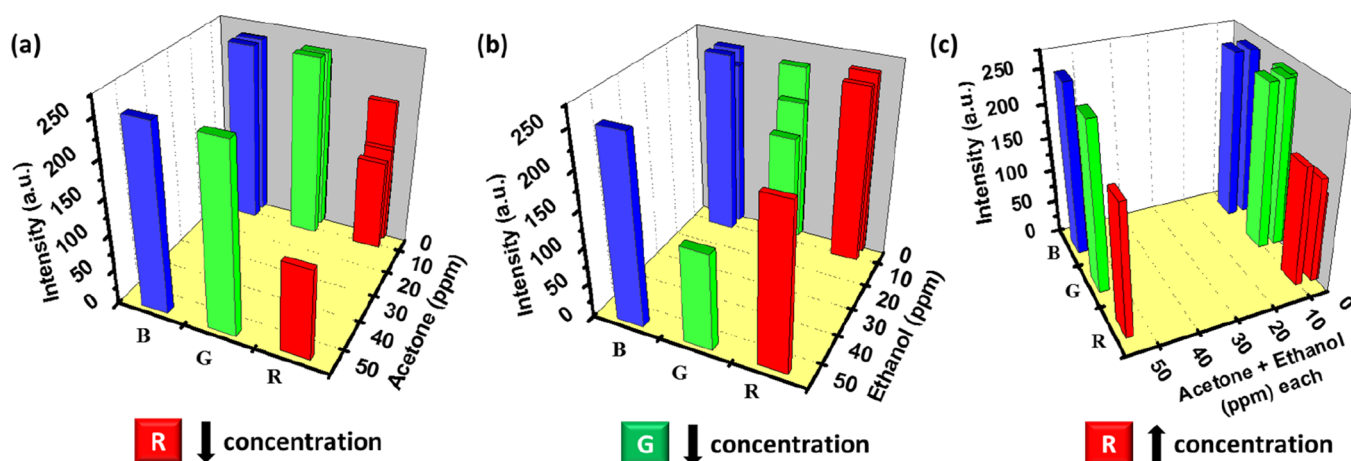


**Figure 8.** Methyl red RGB value plot for detecting different concentrations of (a) acetone, (b) ethanol, and (c) acetone and ethanol simultaneously.

or negligible competition for acetone and ethanol colorimetric detection. Consequently, the dye system is inert to acetone and ethanol detection and displays a potential toward highly selective colorimetric sensor detection.

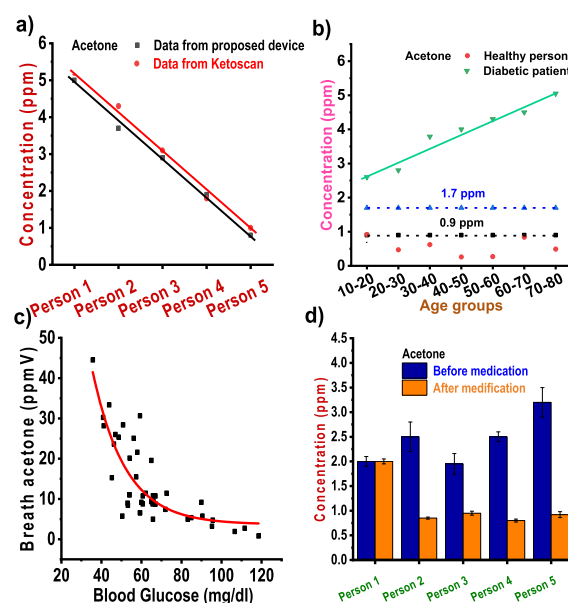
**3.5. Real-Time Evaluation and Comparison of the Prototype.** A portable prototype device with full functions for detecting acetone and ethanol was constructed (Figure 7). Employing the three dyes as the sensing elements, the sensor prototype showed a unique set of RGB values upon exposure to different concentrations (0.05–50 ppm) of biomarkers. Since methyl red detected both acetone and ethanol, the analysis was carried out for different concentrations of (0.05–50 ppm) acetone/ethanol. Both the test solutions were tested in methyl red.

Figure 8 shows plots representing the RGB value associated with different concentrations of the test analyte. For the detection of acetone by methyl red, a decrease in the “R” value was observed with an increase in the concentration (Figure 8a). On the other hand, a decrease in the “G” value was noticed for ethanol sensing with an increase in the concentration (Figure 8b). Interestingly, during the simultaneous detection of acetone and ethanol having an equal concentration in a single-dye solution, an increase in the “R” value was noticed with an increase in concentration (Figure 8c).

Using the developed sensor prototype to analyze the breath of human subjects, we can predict the concentration of acetone/ethanol from the unique RGB value and the trend of change in the value, as shown in Figure 8. Examining the biomarker concentration can reveal the health status of the assessed person.

Real-time evaluation of the proposed device was undertaken to assess the efficacy of a noninvasive assessment of breath. Thirty-five subjects aged between 10 and 80 years were examined based on an acetone concentration of <0.9 ppm in breath to be the usual signature for a healthy individual and a concentration >1.7 ppm, indicating ketoacidosis.<sup>18,19</sup> Human breath samples were analyzed using the colorimetric sensor prototype and compared to a Ketoscan mini-instrument (Figure 9a). Here, the proposed device showed more accuracy compared to the commercial Ketoscan device.

The prevalence of diabetes increases with age, with 3.7% of people in the age group 20–44 years having diabetes, while the number increases to 13.7% for 45–64 years, and is the highest



**Figure 9.** Comparison and evaluation of the proposed colorimetric device. (a) Comparison of data obtained from the proposed device and Ketoscan. (b) Evaluation of the precision of the proposed device in predicting the health status of different age groups. (c) Correlation of breath acetone levels with blood glucose collected from different subjects on their fasting days. (d) Precision of medicine using the proposed device.

(26.9%) in the age group  $\geq 65$  years.<sup>25,26</sup> As age increases, the prevalence of diabetes increases due to the combined effects of increasing insulin resistance and impaired pancreatic islet function with aging.<sup>27</sup> Usually, the detection and monitoring of blood glucose and ketone bodies involve blood tests. This process is painful, invasive, and time-consuming.<sup>28</sup>

We have undertaken real-time experiments by selecting a healthy person and a person with diabetes for each age group and checked the proposed device’s precision to detect acetone concentration (Figure 9b). We also assessed the relationship between acetone and glucose (Figure 9c), which showed a trend for the acetone levels to increase with a decrease in the glucose levels. The data were fitted to an exponentially decaying curve  $Y = A_1 e^{(-x/t_1)} + Y_0$ . The parameters  $A_1$ ,  $t_1$ , and  $Y_0$  were  $333.6498 \pm 170.62379$ ,  $16.39754 \pm 3.57442$ , and

3.681 ± 2.36957, respectively. The squared regression coefficient ( $R^2$ ) was 0.67852. Prabhakar et al. also observed a similar inverse correlation.<sup>29</sup> However, it is important to mention that glucose and acetone are biomarkers reflective of different energy source pathways. Monitoring each metabolic route may provide independent information about the individual's metabolic regulations that depend on glucose availability, glycogen storage, and insulin resistance.

In five patients with diabetes, the acetone concentration was assessed using a colorimetric device before and after taking metformin. The acetone concentrations ranged from 2 to 3 ppm and fell below 0.9 ppm in 4/5 patients (Figure 9d).

These results demonstrate that the proposed device could monitor the production of ketone bodies in subjects who fast, have diabetes, or are treated with SGLT2 inhibitors. Breath acetone measured by colorimetry is more sensitive than blood ketones measured by capillary blood monitors and is noninvasive. Breath acetone assessment could be used to assess ketosis and ketoacidosis. The IoT-based prototype would have a low cost of around \$20, including dye components, whereas other sensors (with lower selectivity, Table 3) cost 10 times higher.

**Table 3. Summary of Various Noninvasive Sensors Used for the Breath Acetone Analysis**

sl. no	sensors	acetone (ppm)	LOD (ppm)	references
1	metal-oxide-based electrochemical sensors	1.5–1000	0.1–0.5	30
2	ultraviolet illumination-assisted sensors	0.6–1	0.1–1	31, 32
3	optical sensors		0.014–5.3	33, 34
4	gas sensors	0.3		35
5	colorimetric sensors		0.65	21
6	present work	0.05	0.02	

The detection of exhaled acetone may also have clinical utility in lung cancer, heart failure, and allergic asthma patients. Acetone is also a significant pollutant in contaminated groundwaters and industrial effluents.

### 3. CONCLUSIONS

A noninvasive colorimetric visual sensor for tracing breath acetone and ethanol in exhaled breath was developed to detect and monitor ketoacidosis. The efficiency of a highly selective multiple-dye system to estimate acetone levels concerning response time, pH effect, temperature effect, and concentration effect was established. A portable and low-cost IoT-based prototype device with full functions for detecting breath biomarkers was constructed by employing the dye solutions as the sensing elements. The successful applications of this novel approach have considerable potential as a visual sensor platform in the biomedical field and the domain of environmental chemistry.

### 4. EXPERIMENTS AND METHODS

**4.1. Materials and Instruments.** Acetone (99.5%), ammonia (25%), benzene (37% w/v), ethanol (99.5%), formaldehyde (99% w/v), formic acid (95%) hydrogen peroxide (30%), iodine, m-cresol purple, methyl orange, and methyl red (2% w/v) were obtained from Sigma-Aldrich along with potassium permanganate (99% w/v), sodium hydroxide,

and toluene (36–40% w/v). All reagents used for analysis were of analytical grade. A millipore Milli-Q water system supplied purified water for the experiment.

UV-VIS spectroscopy characterization was carried by a Biochrom UV spectrophotometer from China with a scanning range of 190–1100 nm. The dyes samples were analyzed in a scanning range of 300–750 nm with a medium scan speed. A step input of 1 nm and a bandwidth of 2 nm were used for characterization.

A Ketoscan instrument by SENTECH GMI, Korea, was used for data evaluation and comparison.

For fabricating the sensors, Arduino UNO, an Adafruit LCD shield (USA), light-emitting diodes (LEDs) (peak around 606 nm), resistors, a TSL230R light-to-frequency sensor, a protoboard, conductors (Cat 5 cable), and a black ABS or PLA filament were used. A QIDI three-dimensional (3D) printer printed the case to protect the sensing elements.

**4.2. Methods.** **4.2.1. Preparation of the Dyes and Characterization.** The methyl red dye solution was prepared by dissolving 50 mg of methyl red in a mixture of 1.86 mL of 0.1 N NaOH and 50 mL of pure ethanol. After the solution was prepared, sufficient water was added to make 100 mL of the dye solution. The second dilution of this dye solution was used for colorimetry. Next, 0.005 N dye solutions of  $\text{KMnO}_4$ , m-cresol purple, and methyl orange were prepared, and the experiments were conducted with the stock solution itself. Finally, 10 mL of these solutions was taken into six vials. The solutions' pH was adjusted to acidic (2, 4, and 6), neutral, and basic (9 and 12) pH. After that, 1 mL of a 50 ppm acetone/ethanol test solution was added to all the dye solutions. A change in color and time was observed for all the dye solutions.

We also used the iodoform test as a technique to detect ethanol. We prepared a mixture containing 25 mL of iodine solution and 10 mL of sodium hydroxide solution, and 5 ppm ethanol was added to it.

The characterizations were carried out using a UV spectrophotometer at room temperature. After the characterization and data assessment, a graph was plotted between absorbance versus wavelength.

**4.2.2. Optimization of Kinetic Parameters.** The dye solutions' pH was adjusted to acidic (2, 4, and 6), neutral, and basic (9 and 12) pH for understanding the effect of pH. Now, 1 mL of the 50 ppm acetone test solution was added to all the dye solutions. A change in color and time was observed for all the dye solutions.

For optimizing the concentration of the biomarkers, test solutions with different concentrations were added to the dye solution at room temperature and a specific pH.

The dye solution–acetone/ethanol mixture was heated at different temperatures, and the temperature effect was also studied at specified pH.

For selectivity analysis, 1 mL of 5 ppm ammonia, benzene, formaldehyde, hydrogen peroxide, nitric oxide, and toluene was added to the dye solutions at room temperature and was observed for the color change. The difference in absorbance was noted for understanding the concentration of the test solution, the temperature of the dye–biomarker mixture, pH, and the selectivity of the dye solutions.

**4.2.3. Indigenously Developed Smartphone-Interfaced Sensor Prototype.** The fabrication procedure of sensitive IoT-based colorimetric sensor prototypes is low-cost and straightforward. We fabricated a 3D printable, open-source colorimeter utilizing only open-source hardware and software



solutions and readily available discrete components. The colorimeter detector assembly was divided into three independent regions, that is, the light source region, sample zone, and color detector area. The light source consisted of four different LEDs, that is, red, blue, white, and green. The light source area was followed by the sample zone, divided into three chambers. Three cuvettes consisting of individual dye solutions were placed sequentially and vertically in each section. The sample zone was protected by a 3D printed protective case and immediately followed the detector zone, including a color detector. The light source, sample zone, and sensor were horizontally aligned to increase the repeatability of obtained results, and the prototype was painted black to minimize reflections. Light from the LED source fell on the three cuvettes consisting of the dye solution and were placed in series one after another. After that, transmitted light from the sample zone was intercepted by the color detector. The detector analyzed the transmitted light and represents the RGB values. Upon exposure to biomarkers, the dye solution changed its color. The detector identified respective color changes in the dye solutions and showed unique RGB values in the device (LCD/smartphone) connected to the sensor prototype through Bluetooth.

## AUTHOR INFORMATION

### Corresponding Author

Kishor Kumar Sadasivuni – Center for Advanced Materials, Qatar University, Doha 2713, Qatar; [orcid.org/0000-0003-2730-6483](https://orcid.org/0000-0003-2730-6483); Phone: (+974) 4403-6686; Email: [kishor\\_kumars@yahoo.com](mailto:kishor_kumars@yahoo.com)

### Authors

Mizaj Shabil Sha – Center for Advanced Materials, Qatar University, Doha 2713, Qatar  
Muni Raj Maurya – Center for Advanced Materials and Department of Mechanical and Industrial Engineering, Qatar University, Doha 2713, Qatar  
Sadiyah Shafath – Center for Advanced Materials and Department of Chemical Engineering, Qatar University, Doha 2713, Qatar  
John-John Cabibihan – Department of Mechanical and Industrial Engineering, Qatar University, Doha 2713, Qatar  
Abdulaziz Al-Ali – Department of Computer Science and Engineering and KINDI Center for Computing Research, Qatar University, Doha 2713, Qatar  
Rayaz A. Malik – Weill Cornell Medicine-Qatar, Qatar Foundation-Education City, Doha 2713, Qatar

Complete contact information is available at: <https://pubs.acs.org/10.1021/acsomega.1c05948>

### Author Contributions

<sup>∇</sup>M.S.S. and M.R.M. are contributed equally.

### Notes

The authors declare no competing financial interest.

## ACKNOWLEDGMENTS

This work was supported by the Qatar National Research Fund under NPRP11S-0110-180247. The statements made herein are solely the responsibility of the authors.

## REFERENCES

- (1) Eledrisi, M. S.; Beshyah, S. A.; Malik, R. A. Management of Diabetic Ketoacidosis in Special Populations. *Diabetes Res. Clin. Pract.* **2021**, *174*, 108744.
- (2) Elhadd, T.; Bashir, M.; Baager, K. A.; Ali, H. A.; Almohannadi, D. H. S.; Dabbous, Z.; Malik, R. A.; Abou-Samra, A.-B. PROFAST Ramadan Study Group. Mitigation of Hypoglycemia during Ramadan Using the Flash Glucose Monitoring System Following Dose Adjustment of Insulin and Sulphonylurea in Patients Taking Multiple Glucose-Lowering Therapies (The PROFAST-IT Study). *Diabetes Res. Clin. Pract.* **2021**, *172*, 108589.
- (3) Gad, H.; Hayat, T.; Al-Muhannadi, H.; Malik, B. R.; Mussleman, P.; Malik, R. A. Efficacy and Safety of the Newer Oral Hypoglycemic Agents in Patients with T2DM during Ramadan: A Systematic Review and Meta-Analysis. *Diabetes Res. Clin. Pract.* **2021**, *172*, 108562.
- (4) Giugliano, D.; Longo, M.; Caruso, P.; Maiorino, M. I.; Bellastella, G.; Esposito, K. Sodium-Glucose Co-Transporter-2 Inhibitors for the Prevention of Cardiorenal Outcomes in Type 2 Diabetes: An Updated Meta-Analysis. *Diabetes Obes. Metabol.* **2021**, *23*, 1672–1676.
- (5) Lu, Y.; Li, F.; Fan, Y.; Yang, Y.; Chen, M.; Xi, J. Effect of SGLT-2 Inhibitors on Cardiovascular Outcomes in Heart Failure Patients: A Meta-Analysis of Randomized Controlled Trials. *Eur. J. Intern. Med.* **2021**, *87*, 20–28.
- (6) Mima, A. Sodium-Glucose Cotransporter 2 Inhibitors in Patients with Non-Diabetic Chronic Kidney Disease. *Adv. Ther.* **2021**, *38*, 2201–2212.
- (7) Mohamed, M. M. G.; Shaikh, S.; Osman, M.; Kheiri, B. Meta-Analysis of Sodium-Glucose Cotransporter 2 Inhibitors in Heart Failure Patients Without Diabetes. *Am. J. Cardiol.* **2021**, *148*, 175–176.
- (8) Qiu, M.; Ding, L.-L.; Zhang, M.; Zhou, H.-R. Safety of Four SGLT2 Inhibitors in Three Chronic Diseases: A Meta-Analysis of Large Randomized Trials of SGLT2 Inhibitors. *Diabetes Vasc. Dis. Res.* **2021**, *18*, 147916412110110.
- (9) Alkabbani, W.; Pelletier, R.; Gamble, J.-M. Sodium/Glucose Cotransporter 2 Inhibitors and the Risk of Diabetic Ketoacidosis: An Example of Complementary Evidence for Rare Adverse Events. *Am. J. Epidemiol.* **2021**, *190*, 1572–1581.
- (10) Kraus, F. B.; Kocijancic, M.; Kluttig, A.; Ludwig-Kraus, B. Test Validation, Method Comparison and Reference Range for the Measurement of  $\beta$ -Hydroxybutyrate in Peripheral Blood Samples. *Biochem. Med.* **2020**, *30*, 118.
- (11) Tang, L.; Chang, S. J.; Chen, C.-J.; Liu, J.-T. Non-Invasive Blood Glucose Monitoring Technology: A Review. *Sensors* **2020**, *20*, 6925.
- (12) Yempally, S.; Hegazy, S. M.; Aly, A.; Kannan, K.; Sadasivuni, K. K. Non-Invasive Diabetic Sensor Based on Cellulose Acetate/Graphene Nanocomposite. *Macromol. Symp.* **2020**, *392*, 2000024.
- (13) Saasa, V.; Beukes, M.; Lemmer, Y.; Mwakikunga, B. Blood Ketone Bodies and Breath Acetone Analysis and Their Correlations in Type 2 Diabetes Mellitus. *J. Diagn.* **2019**, *9*, 224.
- (14) Trefz, P.; Obermeier, J.; Lehbrink, R.; Schubert, J. K.; Miekisch, W.; Fischer, D.-C. Exhaled Volatile Substances in Children Suffering from Type 1 Diabetes Mellitus: Results from a Cross-Sectional Study. *Sci. Rep.* **2019**, *9*, 15707.
- (15) Reinhart, J. Early Detection of Diabetic Ketoacidosis by Breathalyzer in a Sailor Reporting for Duty. *Mil. Med.* **2019**, *184*, e951–e952.
- (16) Fayfman, M.; Pasquel, F. J.; Umpierrez, G. E. Management of Hyperglycemic Crises: Diabetic Ketoacidosis and Hyperglycemic Hyperosmolar State. *Med. Clin. North Am.* **2017**, *101*, 587–606.
- (17) Saasa, V.; Malwela, T.; Beukes, M.; Mokgotho, M.; Liu, C.-P.; Mwakikunga, B. Sensing Technologies for Detection of Acetone in Human Breath for Diabetes Diagnosis and Monitoring. *J. Diagn.* **2018**, *8*, 12.
- (18) van Keulen, K. E.; Jansen, M. E.; Schrauwen, R. W. M.; Kolkman, J. J.; Siersema, P. D. Volatile Organic Compounds in Breath Can Serve as a Non-Invasive Diagnostic Biomarker for the Detection

of Advanced Adenomas and Colorectal Cancer. *Aliment. Pharmacol. Ther.* **2020**, *51*, 334–346.

(19) Mitraryana; Apriyanto, D. K.; Satriawan, M. CO<sub>2</sub> Laser Photoacoustic Spectrometer for Measuring Acetone in the Breath of Lung Cancer Patients. *Biosensors* **2020**, *10*, 55.

(20) Maurya, M. R.; Onthath, H.; Morsy, H.; Riyaz, N.-U. -S.; Ibrahim, M.; Ahmed, A. E.; Abuznad, R.; Alruwaili, A.; Alsaedi, F.; Kasak, P.; Sadasivuni, K. K. Colorimetry-Based Detection of Nitric Oxide from Exhaled Breath for Quantification of Oxidative Stress in Human Body. *Healthcare* **2021**, *9*, 1055.

(21) Wang, D.; Zhang, F.; Prabhakar, A.; Qin, X.; Forzani, E. S.; Tao, N. Colorimetric Sensor for Online Accurate Detection of Breath Acetone. *ACS Sens.* **2021**, *6*, 450–453.

(22) Prabhakar, A.; Quach, A.; Zhang, H.; Terrera, M.; Jackemeyer, D.; Xian, X.; Tsow, F.; Tao, N.; Forzani, E. S. Acetone as Biomarker for Ketosis Buildup Capability - a Study in Healthy Individuals under Combined High Fat and Starvation Diets. *Nutr. J.* **2015**, *14*, 41.

(23) Galassetti, P. R.; Novak, B.; Nemet, D.; Rose-Gottron, C.; Cooper, D. M.; Meinardi, S.; Newcomb, R.; Zaldivar, F.; Blake, D. R. Breath Ethanol and Acetone as Indicators of Serum Glucose Levels: An Initial Report. *Diabetes Technol. Therapeut.* **2005**, *7*, 115–123.

(24) Gamella, M.; Campuzano, S.; Manso, J.; Rivera, G. G. d.; López-Colino, F.; Reviejo, A. J.; Pingarrón, J. M. A Novel Non-Invasive Electrochemical Biosensing Device for in Situ Determination of the Alcohol Content in Blood by Monitoring Ethanol in Sweat. *Anal. Chim. Acta* **2014**, *806*, 1–7.

(25) Sonner, Z.; Wilder, E.; Heikenfeld, J.; Kasting, G.; Beyette, F.; Swaile, D.; Sherman, F.; Joyce, J.; Hagen, J.; Kelley-Loughnane, N.; Naik, R. The Microfluidics of the Eccrine Sweat Gland, Including Biomarker Partitioning, Transport, and Biosensing Implications. *Biomicrofluidics* **2015**, *9*, 031301.

(26) Munje, R. D.; Muthukumar, S.; Panneer Selvam, A.; Prasad, S. Flexible Nanoporous Tunable Electrical Double Layer Biosensors for Sweat Diagnostics. *Sci. Rep.* **2015**, *5*, 14586.

(27) ACS Sensors. Noninvasive Alcohol Monitoring Using a Wearable Tattoo-Based Iontophoretic-Biosensing System, <https://pubs.acs.org/doi/10.1021/acssensors.6b00356> (accessed Sept 26, 2021).

(28) Noh, J.-W.; Jung, J. H.; Park, J. E.; Lee, J. H.; Sim, K. H.; Park, J.; Kim, M. H.; Yoo, K.-B. The Relationship between Age of Onset and Risk Factors Including Family History and Life Style in Korean Population with Type 2 Diabetes Mellitus. *J. Phys. Ther. Sci.* **2018**, *30*, 201–206.

(29) Prabhakar, A.; Quach, A.; Wang, W.; Terrera, M. Breath Acetone as Biomarker for Lipid Oxidation and Early Ketone Detection. *Global J. Obes. Diabetes, Metab. Syndrome* **2014**, *1*, 103.

(30) Rydosz, A. Sensors for Enhanced Detection of Acetone as a Potential Tool for Noninvasive Diabetes Monitoring. *Sensors* **2018**, *18*, 2298.

(31) Yang, C.-M.; Chen, T.-C.; Yang, Y.-C.; Hsiao, M.-C.; Meyyappan, M.; Lai, C.-S. Ultraviolet Illumination Effect on Monolayer Graphene-Based Resistive Sensor for Acetone Detection. *Vacuum* **2017**, *140*, 89–95.

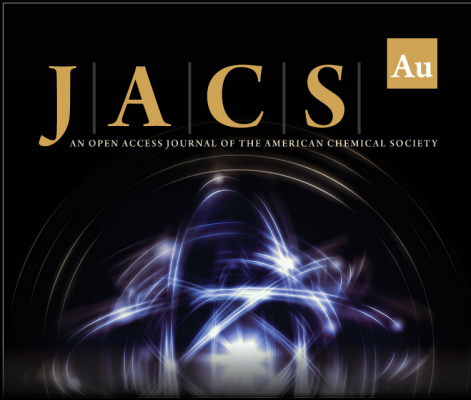
(32) Zhang, H.; Qin, H.; Zhang, P.; Chen, Y.; Hu, J. Low Concentration Acetone Gas Sensing Properties of 3 Wt% Pd-Doped SmCo<sub>x</sub>Fe<sub>1-x</sub>O<sub>3</sub> Nanocrystalline Powders under UV Light Illumination. *Sensor. Actuator. B Chem.* **2017**, *260*, 33.

(33) Ye, M.; Chien, P.-J.; Toma, K.; Arakawa, T.; Mitsubayashi, K. An Acetone Bio-Sniffer (Gas Phase Biosensor) Enabling Assessment of Lipid Metabolism from Exhaled Breath. *Biosens. Bioelectron.* **2015**, *73*, 208–213.

(34) Deng, C.; Zhang, J.; Yu, X.; Zhang, W.; Zhang, X. Determination of Acetone in Human Breath by Gas Chromatography-Mass Spectrometry and Solid-Phase Microextraction with on-Fiber Derivatization. *J. Chromatogr. B: Anal. Technol. Biomed. Life Sci.* **2004**, *810*, 269–275.


(35) Chuang, M.-Y.; Lin, Y.-T.; Tung, T.-W.; Chang, L.-Y.; Zan, H.-W.; Meng, H.-F.; Lu, C.-J.; Tao, Y.-T. Room-Temperature-Operated


Organic-Based Acetone Gas Sensor for Breath Analysis. *Sensor. Actuator. B Chem.* **2018**, *260*, 593.



**JACS** Au  
AN OPEN ACCESS JOURNAL OF THE AMERICAN CHEMICAL SOCIETY

Editor-in-Chief  
**Prof. Christopher W. Jones**  
Georgia Institute of Technology, USA

**Open for Submissions** 

pubs.acs.org/jacsau  ACS Publications  
Most Trusted. Most Cited. Most Read.